CSCanada
Advances in Petroleum Exploration and Development
Vol. 16, No. 1, 2018, pp. 49-71
DOI:10.3968/10614

ISSN 1925-542X [Print]
ISSN 1925-5438 [Online]
www.cscanada.net
www.cscanada.org

Prediction Modeling for Combination Drive Reservoir Performance

Mohamed Halafawi[a],*; Abdel Waly Abdalah Abdel Waly[b]

[a]Teacher assistant. Petroleum Engineering, Cairo University, Giza, Egypt.
[b]Professor. Petroleum Engineering, Cairo University, Giza, Egypt.
*Corresponding author.

Received 19 June 2018; accepted 8 September 2018
Published online 26 September 2018

Abstract

Depletion performance of combination drive oil reservoirs is highly influenced by changes in reservoir rock and fluid data, relative permeability data, and PVT data of reservoir. Therefore, future prediction of combination drive oil reservoirs is difficult due to the long terms, huge equations and the sensitivity of data especially the PVT data and relative permeability data.

In this paper, an integrated analytical model was developed to simulate the combination drive oil reservoir's performance. It couples the general material balance equation with equations for water influx, water-invaded pore volume, gas-invaded pore volume, oil and gas saturation, and fluid contacts for combination oil reservoirs. All these equations are merged and solved simultaneously with reservoir depletion stages.

A comparison with the various equations' results for the integrated model has been developed so that it can be utilized in history match mode. This is used to estimate fluid saturation distribution after water influx and gas-cap invasion, original fluids in place, aquifer parameters and type, fluid contact levels, and effective recovery factor during gas and water aquifer movement towards the productive hydrocarbon zone in all reservoir depletion stages.

The developed model has been validated using published cases for various oil reservoirs' conditions, resulting in a good match between published case results and developed model results for these reservoirs. After validating the model, it has been used for two Egyptian combination drive fields. The field production history has been matched and future production performance for these reservoirs was simulated.

Finally, the developed model also has the capability to predict reservoir performance for another Egyptian combination drive oil reservoir field under water and or gas injection, integrated with decline curve analysis.

Key words: Combination drive reservoirs; History match; Future performance prediction; Injection performance; Fields case studies; Prediction model

Halafawi, M., & Abdel Waly, A. A. (2018). Prediction Modeling for Combination Drive Reservoir Performance. *Advances in Petroleum Exploration and Development*, *16*(1), 49-71. Available from: http://www.cscanada.net/index.php/aped/article/view/10614
DOI: http://dx.doi.org/10.3968/10614

INTRODUCTION

Depletion drive, gas-cap drive, water drive, gravity drainage drive, and rock-liquid expansion drive are the mechanisms that provide the natural energy necessary for oil recovery. Some of the reservoirs may produce under the influence of a combination of these drives and are designated as "combination drive reservoirs." Additionally, a secondary gas-cap forms due to gravitational forces, which may favor the segregation of fluids, thus tending to shorten the transition zone between oil and displacing fluids. At the end, a weak gas-cap combination drive reservoir is formed.

Recently, some of the discovered fields in the Middle East, the Mediterranean Sea, and the North Sea are combination drive reservoirs. Many petroleum engineering experts have posited the discoveries of the well-known reservoirs have nearly reached their end. Thus, it is now time to explore the unknown ones such as combination reservoirs. This means that all these new reservoirs would require developing new models to be fully studied and analyzed so that the best history match

and future performance prediction could attained.

However, these kinds of reservoirs require high depletion and future performance studies so that development plans and management decisions could be taken based on considerable, technical, accurate, and motivated ways. Therefore, all attempts to extend the Terner and Muskat prediction methods (Craft, & Hawkins, 1991) to include the combination drive case would result in a divergence between future performance predictions and misleading results. Wooddy & Moscrip (1956) studied the performance calculations for combination drive reservoirs only from the saturation point of view while Saleh (Saad, 1990) developed the performance calculation model for a partial combination drive reservoir that contained only gas and water. In addition, Exxon (1978) presented the history match assuming unsteady state water influx and future performance from saturation point of view for the combination reservoir. On the other hand, Smith, Tracy and Farrar (1992) showed a simple depletion performance example assuming steady state water influx for these kinds of reservoirs. Kirby, Stamm and Schnitz (1956) also studied the depletion history, future performance, and injection performance of a gas-cap-drive reservoir.

Delauretis, Yarranton, and Baker (2008) also showed the application of material balance and volumetrics to determine reservoir fluid saturations and fluid contact levels for various reservoirs including a combination drive. Moreover, there are some authors who presented developed methods for obtaining original fluids in place and aquifer parameters from material balance equation by improving the solution of Havlena and Odeh (Havlena & Odeh, 1963; Havlena & Odeh, 1964), also applying mathematical elements such as curve fitting to determine the best accurate parameters. It is worth mentioning that all the previous authors have assumed the same when applying their techniques or methods. These assumptions are concerning the material balance and water influx such as: homogeneous, isotropic reservoir, uniform thickness, no tonguing or coning, constant and uniform properties, constant reservoir temperature, constant reservoir volume, and the other assumptions listed by the previous authors. Therefore, it is better for the developed model to stick to these assumptions so that contradictions do not occur. However, partial homogeneity has been taken into consideration because of the displacement and sweep efficiencies changes (Welge, 1952). Thus, the demand for a model to study the depletion and predict the combination drive reservoirs performance became extensively desirable.

Obviously, the use of general material balance equation (MBE), coupled with the suitable water influx model equations (WIM) was helpful for history match in determining OOIP, OGIP and aquifer parameters (C, r_D, and aquifer model: steady state, unsteady state, or pseudo steady state).

However, in case of unsteady state, the water influx tables' lookup and interpolation approach has several drawbacks (Klins, Bouchard, & Cable, 1988) including interpolation inaccuracy, lengthy calculation times, and programming difficulties. Thus, Klins, Bouchard and Cable (1988) developed a polynomial approach to the van-Everdingen-Hurst (Van Everdingen & Hurst, 1949) dimensionless water encroachment variables of pressure and rate, which were used in the developed model. In addition, due to the fact that aquifer size ratio and dimensionless time are implicit, no interpolation is needed. These analytical expressions are also applicable to aquifer/reservoir ratios of 25:1(Klins, Bouchard, & Cable, 1988).

For the long term production, the approach of Havlena and Odeh (1963, 1964) considering the material balance equation as a straight line was used to determine the OOIP, OGIP and Aquifer constant. The historically estimated parameters were then used to forecast combination drive reservoir performance under producing oil, gas, and water.

The developed model allows the calculation of volumetric changes of fluids in the gas cap, oil zone, and aquifer during fluctuating withdrawals and reservoir pressures. It provides a means for determining reservoir fluid distribution changes corresponding to these volumetric changes. A certain amount of knowledge of reservoir fluid saturation distribution at various stages of depletion is necessary in order to determine the recovery efficiency of gas and water, permitting the reliable prediction of ultimate oil recovery.

The described model procedures have been used satisfactorily to analyze past performance and predict future behavior of combination drive reservoirs under either primary or pressure-maintenance operations. These procedures include the calculations of material balance parameters, water influx parameters, fluids' saturations distribution, fluids' contact levels, recovery factors, and fluids' efficiency.

The objective of that model is to develop a technique to predict reservoir performance in combination drive type. Firstly, the most suitable aquifer model must be selected and it's parameters determined. Secondly, history match needs to be implemented. Thirdly, comparisons between the various equations and the most applicable equations should be selected for future performance. Finally, the selected aquifer model is utilized along with the selected future reservoir performance equations. However, it is necessary to determine cumulative oil field production (Np), cumulative gas field production (Gp) and cumulative water production (Wp) for future intervals. Two methods will be used to determine them: Firstly, The decline curve analysis (DCA) method (Fetkovich, Fetkovich, & Fetkovich, 1994) is used to predict ΔNp and assure with the HCV-Depth curve's ΔNp Value. Secondly, the plot of the production history versus time is helpful to take the future value of N_p from the trend line of water oil

ratio (WOR vs. time) as a close value of N_p.

1. DEVELOPED MODEL

To satisfy the objective of being able to run the developed model to match historical production and predict future performance, it is necessary to describe reservoir rock and fluid data, PVT data, relative permeability data, pressure viscosity data, and pressure production data. This model needs to select the most suitable PVT, relative permeability and viscosity equations that were presented by Craft, Hawkins (1991), Smith, Tracy, Farra (1992), and Tarek (2006) for future prediction. In addition, the sensitivity analyses for the selected PVT, relative permeability and viscosity correlations should be implemented before predictions. Thus, the following sections describe material balance, aquifer model, Gas/Oil Ratio (GOR), saturation, injection, fluid contacts, and recovery factor equations.

1.1 Material Balance Equation

Material balance equation used to calculate water influx (Craft & Hawkins, 1991; Exxon, 1978; Smith et al., 1992; Tarek, 2006):

$$We=N_p[\beta_o+(R_{poz}-R_{si})\beta_g]+W_p\beta_{wp}-N[(R_{si}-R_s)\beta_g+(\beta_{oi}-\beta_o)]-[G(\beta_g-\beta_{gi})-G_{pc}\beta_g] \quad (1)$$

1.2 Aquifer Model

The type of aquifer model affects reservoir performance as the aquifer parameters must first be known so this piece of information can be used in future performance description. The different water influx models (Tarek, 2006) commonly used in petroleum reservoir studies include Pot aquifer model, Schilthuis' steady-state (Schilthuis, 1936), Hurst's modified steady-state (Hurst, 1943), Van Everdingen-Hurst unsteady-state (Van Everdingen & Hurst, 1949) (edge-water drive and bottom-water drive), Carter-Tracy unsteady-state (Carter & Tracy, 1960), Fetkovich's method (Fetkovich, 1971) (radial aquifer and linear aquifer) and others numerical models. Below are the most commonly used aquifer models:

Steady State Equation **(Schilthuis, 1936)**:

$$W_e=C\,\Sigma\Delta P\Delta t \quad (2)$$

Un-Steady State Equation **(Van Everdingen & Hurst, 1949)**:

$$W_e=C\,\Sigma\Delta PQ_{tD} \quad (3)$$

$$C=1.119\varphi h\,C_{wr}R_o^{\,2}f \quad (4)$$

$$\Delta P=\frac{P_{j-1}-P_{j+1}}{2} \quad (5)$$

Pseudo-Steady State Equation **(Fetkovich, 1971)**:

$$W_e=\frac{W_{ei}}{P_i}(P_i-P_R)\left(1-e^{-\frac{I\,P_i t}{W_{ei}}}\right) \quad (6)$$

1.3 Gas/Oil Ratio (GOR) Equation

The produced gas-oil ratio is the ratio of total produced gas to produced oil. The instantaneous gas-oil ratio can be expressed mathematically as follows (Craft & Hawkins, 1991; Smith et al., 1992; Tarek, 2006):

$$GOR=R_s+\left(\frac{K_{rg}}{K_{ro}}\right)\left(\frac{\mu_o\beta_o}{\mu_g\beta_g}\right) \quad (7)$$

1.4 Saturation Equations

Oil saturation for a combination-drive reservoir that can be adjusted to account for both driving mechanisms was calculated as follows (Tarek, 2006):

$$S_o=\frac{(N-N_p)\beta_o-\left[\frac{Nm\beta_{oi}\left(\frac{\beta_g}{\beta_{gi}}-1\right)S_{org}}{1-S_{wi}-S_{org}}+\frac{(W_e-W_p\beta_w)S_{orw}}{1-S_{wi}-S_{orw}}\right]}{\frac{N\beta_{oi}}{1-S_{wi}}-\left[\frac{Nm\beta_{oi}\left(\frac{\beta_g}{\beta_{gi}}-1\right)}{1-S_{wi}-S_{org}}+\frac{(W_e-W_p\beta_w)}{1-S_{wi}-S_{orw}}\right]} \quad (8)$$

For calculation of gas and oil saturations in the remaining oil zone (un-invaded zone) at the end of any period, Wooddy equations are used (Wooddy & Moscrip, 1956):

$$S_{g\omega}=\frac{S_{g\omega(j-1)}\frac{B_g}{B_{g(j-1)}}+\left[\left(\frac{S_{o\omega}}{B_o}\right)_{j-1}+\left(\frac{1-S_{wc}}{B_o}\right)_j\right]\left[\left(\frac{B_t-B_o}{B_{ti}}\right)_j-\left(\frac{B_t-B_o}{B_{ti}}\right)_{j-1}\right]\frac{B_g}{2}}{1+\left[\left(\frac{B_t-B_o}{B_{ti}}\right)_j-\left(\frac{B_t-B_o}{B_{ti}}\right)_{j-1}\right]\frac{B_g}{2B_o}}+\frac{\left[\frac{0.044\overline{K_g}A_\omega}{5.615\mu_g}\left(\Delta\bar{p}-\frac{144\Delta P}{h}\right)\Delta\theta\,(\sin\alpha)\frac{B_g}{B_o}+\frac{K_{ro}\bar{\mu}_o}{K_{rg}\bar{\mu}_g}(\Delta N_{p\omega}B_oB_{ti})\frac{B_g}{B_g}\right]}{\frac{\varphi A_\omega L_\omega}{5.615}\left(1+\frac{\left[\left(\frac{B_t-B_o}{B_{ti}}\right)_j-\left(\frac{B_t-B_o}{B_{ti}}\right)_{j-1}\right]B_g}{2B_o}\right)} \quad (9)$$

Saleh's equation used for calculating oil saturation in oil zone (Saad, 1990):

$$S_{oj}=\frac{(N-N_p-N_{tw}-N_{tg})\beta_{oj}}{\frac{N\beta_{ti}}{1-S_{wi}}-\sum_{i=1}^{j}\Delta V_{wi}-\sum_{i=1}^{j}\Delta V_{gi}} \quad (10)$$

Where

$$N_{tw}=\sum_{i=1}^{j}\Delta V_{wi}\frac{Sorwi}{\beta_{oi}} \quad (11)$$

$$N_{tg}=\sum_{i=1}^{j}\Delta V_{gi}\frac{Sorgi}{\beta_{oi}} \quad (12)$$

Smith's equation for saturation in the remaining oil zone in a combination-drive reservoir (Smith et al., 1992):

$$S_o=\frac{(N-N_p)\beta_o-(GCE)(S_{org})-(WCM)(S_{orw})}{\frac{N\beta_{oi}}{1-S_{wc}}-(GCE+WCM)} \quad (13)$$

Where

$$GCE=\frac{G(\beta_g-\beta_{gi})-G_{pc}\beta_g+Q_{gin}\beta_g}{S_{gavg}} \quad (14)$$

$$WCM=\frac{W_e-W_p\beta_w+W_{in}}{S_{gavg}-S_{wc}} \quad (15)$$

To calculate the residual oil saturation in water invaded zone (S_{orw}) Naar and Henderson (1961) formula was used, where the displacement is produced imbibition in the presence of free gas saturation as follows:

$$S_{orw}=\frac{1}{2}(1-S_{wi})\left(\frac{S_{oi}}{1-S_{wi}}\right)^2 \quad (16)$$

The Welge (1952) method based on the Buckley and Leverett flow relationship for immiscible fluids is also

recommended for general use in calculating the residual oil saturation in water invaded zone (S_{orw}):

$$f_d = \frac{\frac{\mu_o}{\mu_d}}{\frac{\mu_o}{\mu_d}+\frac{K_{ro}}{K_{rd}}} - \frac{0.488 \times 10^{-3} A K K_{ro} |\Delta\gamma| \sin\alpha_d}{q_t \mu_d \left[\frac{\mu_o}{\mu_d}+\frac{K_{ro}}{K_{rd}}\right]} \quad (17)$$

1.5 Fluid Contacts Equations

The Gas-Oil Contact (GOC) and the Oil-Water Contact (OWC) were calculated by Saleh's set of equations (Saad, 1990):

$$\Delta hw=(Ro-Roc)\sin\theta \quad (18)$$

Where

$$R_{oc}=\sqrt{R_o^2 - \frac{\Delta V_{wj}}{\psi n H \varphi x 5.615}} \quad (19)$$

And

$$\Delta h_g=(R_{gc}-R_{gi})\sin\theta \quad (20)$$

Where

$$R_{gc}=\sqrt{R_{gi}^2 - \frac{\Delta V_{gj}}{\psi n H \varphi x 5.615}} \quad (21)$$

Delauretis et al. equations that describe the remaining gas, oil and water volumes, respectively, during reservoir depletion were used as follows (Delauretis, Yarranton, & Baker, 2008):

$$PV_{GOC} = \left\{\frac{N(R_{si}-R_s)\beta_g - N_p(R_p-R_s)\beta_g + \frac{N m \beta_{oi}}{\beta_{gi}}\beta_g + G_I\beta_{ig} - (PV_{OGOC})S_{org} - (PV_{BWOC})S_{gc}}{(1-S_{wi}-S_{org}-S_{gc})}\right\} \quad (22)$$

$$PV_{WOC}=PV_{BWOC}-\left[\frac{W_e\beta_w - W_p\beta_w + W_I\beta_{iw}}{(1-S_{org}-S_{gc})}\right] \quad (23)$$

1.6 Decline Curve Analysis (DCA) Equation

Two methods, as mentioned before, will be used to determine Np and Gp. One of them is DCA method that will also be used to predict ΔNp and assure the HCV-Depth curve's ΔNp Value. The DCA method (Fetkovich, Fetkovich, & Fetkovich, 1994) can be summarized as follows:

- Use conventional decline curve analysis for production data
- Fit exponential, harmonic decline or hyperbolic decline with production data
- Match past performance
- Forecast future performance

The Arps equation, used to get equations for different decline, is:

$$q(t)=\frac{qi}{(1+bD_it)^{1/E}} \quad (24)$$

Where b = 0 for exponential decline, b = 1 for harmonic decline, and 0 < b < 1 for the general case of hyperbolic decline.

1.7 Injection Equations

Injection equations used to build the developed model vary. They include Cole's equations for calculating gas-cap shrinkage and amount of oil lost due to gas-cap shrinkage (Cole, 1969):

$$\text{Oil Lost} = \frac{\left[G_{pc}\beta_g - N\,m\,\beta_{oi}\left(\frac{\beta_g}{\beta_{gi}}-1\right)\right]S_{org}}{(1-S_{wi}-S_{gr})\beta_{oa}} \quad (25)$$

$$G_{inject}=\text{Gas-Cap Shrinkage}=G_{pc}\beta_g - N m \beta_{oi}\left[\frac{\beta_g}{\beta_{gi}}-1\right] \quad (26)$$

These equations are used to ascertain the quantity of gas needed to reach full pressure maintenance assuming total produced water will be injected back into reservoir. In addition, Kirby, Stamm and Schnitz (1956) have presented equations for evaluating gas-cap drive performance under full pressure maintenance by gas injection and water injection. Their equations are shown below:

$$\frac{\Delta G_i}{\Delta t}=\frac{\Delta N_p}{\Delta t}\frac{\beta_o\beta_{ti}}{\beta_g} + \frac{\Delta N_{po}}{\Delta t}\frac{\overline{K_g}}{\overline{K_o}}\frac{\overline{\mu_o}}{\overline{\mu_g}}\frac{\beta_o\beta_{ti}}{\beta_g} + \frac{\Delta G_{pc}}{\Delta t} \quad (27)$$

$$\frac{\Delta G_{i(ext)}}{\Delta t}=\frac{\Delta N_p}{\Delta t}\left(\frac{\beta_o\beta_{ti}}{\beta_g} - \frac{R_s}{1000}\right) \quad (28)$$

$$\frac{\Delta W_i}{\Delta t}=\frac{\Delta N_p\beta_o\beta_{ti}}{\Delta t} + \frac{\Delta N_{po}\beta_o\beta_{ti}}{\Delta t}\frac{\overline{K_g}}{\overline{K_o}}\frac{\overline{\mu_o}}{\overline{\mu_g}} + \frac{\Delta G_{pc}}{\Delta t} + \frac{\Delta W_p}{\Delta t} \quad (29)$$

$$\frac{\Delta W_{i(ext)}}{\Delta t}=\frac{\Delta W_i - \Delta W_p}{\Delta t} \quad (30)$$

Moreover, all previous equations can be adjusted to include the injection terms. Material balance can also be used in terms of drive indices to indicate the effects of injection.

2. MODEL PROCEDURES

Figure A-1 shows the developed integrated model general procedures that include three sections:

- Run the history match model to estimate OOIP, OGIP, aquifer parameters (r_D, C), RF,HCV-depth curve, and saturations distribution.
- Run the sensitivity analyses for PVT correlations and relative permeability correlation to select the best correlation.
- Run the performance prediction model to show future reservoir performance
- Run the injection performance model and show it's effect on recovery

Details about the procedures are included in appendix (A) with flow charts from figures A-2 to A-5.

3. MODEL APPLICABILITY

3.1 Case (1) Published field

Data for the field was published in Exxon (1978). The pressure-production history is summarized in table B-1. Neither water, nor gas-cap has been produced. Reservoir rock and fluid data are listed in table B-2. The production

rate for future operations will be assumed constant at 60,000 STB/D. Prediction will be done for five periods. Each period is taken as half a year.

3.2 Case (2) An Egyptian Combination Drive Oil Field (Injection Application)

The production history and it's dynamic description of X-field are shown in figure B-1. The field shows two phases of steady decline separated by an anomalous change in rate and water cut during June 1993. It is not clear if the cause of this event was geological or mechanical. Uncertainties related to production allocation within the complex formation (which X-field is tied back to) do not allow us to make a definitive interpretation of what occurred. The X-field -1st. discovery well was drilled in 1980 to the primary target. Initial DST flowed 4470 BOPD with GOR ~2940 SCF/STB & API° = 47-54. After isolating the primary gas cap, a second DST flowed 2888 BOPD with GOR ~985-1070 and API° = 34.

However, given the lack of any obvious engineering change or intervention in the field records, and that of the complex formation that would explain the instantaneous increase in production and drop in water cut, it is reasonable to assume that this was a geological event related to the hydraulic breakdown of the fault separating the two primary reservoir compartments (west from east) as shown in the depth and structure map in figure B-2 through figure B-3. Prediction will be done for more than six periods by combining material balance with DCA. In addition, statistical analyses for reservoir performance prediction under injection would be implemented.

3.3 Case (3) Another Egyptian Combination Drive Oil Field

A recent combination drive of the Egyptian field discovered in 2006 with available pressure-production history from 2006 to 2011 is summarized in table B-3. The production rate for future operations will be assumed constant at 200 STB/D for oil, 2 MMSCFD for gas, and 600 STB/D for water. Water and gas-cap have been produced. Reservoir rock and fluid data are listed in table B-4. Structure contour map is shown in figure B-4. Prediction was done for three years.

4. ANALYSIS OF THE RESULTS

4.1 Case (1) Published field

Historical analysis for published case (1) of combination drive oil reservoir with small gas cap and large aquifer resulted in OOIP=438.86 MMSTB and OGIP= 191.17 BSCF. The aquifer parameters from the developed model as shown in figure C-1 are aquifer constant (C)=~ 6900 and the dimensionless radius ($r_D = r_{aquifer} / r_{reservoir}$)= 9.8, compared with the actual published data where ((C) =~ 7000 & r_D = 10). The model has a good match with published data (figure C-1).

Water and gas displacement resulted in invaded zones by gas and water and the saturation distribution in all reservoir changes. Calculations for saturation distribution were implemented (figures C-2 & C-3) for case (1). For all these figures, the Welge method - based on Buckley and Leverett equation - shows more reliable values for average water saturation in water invaded zone (S_{wavg} = 82%) and average gas saturation in gas invaded zone (S_{gavg}= 66%). In addition, it also gives more accurate results for residual saturation of water (S_{orw}= 17.5%) and of gas invasion (S_{org}= 14.5%)

It is clear that recovery by displacement, mostly water and gas drive, is an important drive mechanism. Thus, the effective recovery factor was found roughly constant during pressure decline within oil zone (RF_{eff}= 45 %) (figure C-4). Integrating pore volume equations with radius of contacts equations has resulted in the HCV versus depth volume curve shown in figures C-5 & C-6. A comparison was established between these two curves and evaluate against similar logged results to get an accurate value for the m ratio (m= 0.302441).

Assuming the production rate for future operations will be 60,000 STB/D, future prediction performance appears in predicting pressure versus time compared with IMBAL commercial software. A confirmation of water influx by MBE and the aquifer model was performed. Also, produced GOR was confirmed. As shown in figure C-7 for published case (1), the pressure performance for future interval decreases gradually with time and the predicted values show a good match with that obtained from IMBAL software. The first check on water influx (figure C-8) case (1) has illustrated a good match between $\mathbf{W_e}$ from MBE and $\mathbf{W_e}$ from aquifer model. A small difference between two water influx curves and that of IMBAL software has appeared. The second check on the produced GOR as in figure C-9 published case (1) has also showed a good match between the two curves. The difference between these curves and that of IMBAL software is related to the gas saturation used in IMBAL, which is the average gas saturation in the entire reservoir. This contrasts the GOR equation, which depends on free gas in the un-invaded zone. The discrepancy between the two is due to the tank assumption of IMBAL, which allows gas to be produced from gas cap and un-invaded oil zone.

As stated in the published research, the absolute error in GOR to be taken into consideration is less than 10%. Trial and error estimates were made to get that ratio (figure C-10). The obtained percentage of error is less than 5 % as opposed to 10 % and decreases in future intervals to less than 5 %.

4.2 Case (2) An Egyptian Combination Drive Oil Field (Injection Application)

The application of decline curve analysis and HC-plot in both fault sides with the integrated model proved to

be extremely successful as illustrated in the results of the second Egyptian combination field case (2) appendix (C) which are shown in figures C-11 through C-14. The basis of the current Proved Reserves estimate (PDP) is decline curve analysis, as it is appropriate for a mature conventional oil producing field with a long history of trendable production data. The production period from 1993 to 2009 has been used as part of the decline analysis. An exponential decline has been resulted as shown in figure C-12 (A&B). For worst-case scenario of depletion, initial decline from western fault block would deliver 7 MMbbl oil but post-93 decline would add 4 MMbbl oil from the eastern fault block.

The latest well proved communication between the eastern and western fault blocks based on MDT (Modular Dynamic Tester) pressures was taken while drilling. There is upside oil volume should the original oil water contact lie significantly below the ODT level of 2806m as in figure B-3 through figure B-4. The reservoir prediction performance appeared in production rates performance of figure C-12 (A&B) with an increase in reserve of figure C-13, and an increase in the recovery factor during secondary recovery while gas and water injections are resulted. Thus, resulting in an effective recovery factor of 35% is shown in figure C-14. Firstly, DCA has resulted in an exponential decline for pressure performance and an exponential decline for production oil rates with decline 7.48%, cumulative oil production at beginning of forecasting 10545290 bbl, remaining reserve 1020171 bbl, and for forecasting reservoir would produce for another 15.1 years to reach to 39.1 years as a maximum period of production (figures C-12 (A&B) and C-14). On the other hand, statistical analysis for reservoir performance prediction under injections has been implemented. The study analysis has resulted in increasing RF during water injection, gas injection or both and it has also resulted in an effective recovery factor of 35% (figure C-14).

4.3 Case (3) Another Egyptian Combination Drive Oil Field

The concept of Havelena and Odeh, used for another Egyptian combination drive oil reservoir with a huge gas cap and weak aquifer, has resulted in OOIP=8 MMSTB and OGIP= 30 BSCF as shown in figure C-15. The aquifer parameters resulting from the developed model are (C) =~ 0.0423 and infinite (rD>>25) unsteady state model. It is clear that recovery by displacement, mostly gas drive, is the most effective drive mechanism. Thus, the effective recovery factor has appeared nearly stationary during pressure decline within oil zone (RFeff= 65%) with a great share from the effect of gas cap (figure C-18).

Calculations for saturation distribution in a reservoir were made for the Egyptian field case (3) illustrated in figure C-16 and figure C-17. For all these figures, the Welge method - based on Buckley and Leverett equation has proven more reliable for average water saturation in water invaded zone (S_{wavg} = 80%), and average gas saturation in gas invaded zone (S_{gavg}=70%). It has also produced more accurate results for residual saturations of gas invasion (S_{orw} =21%) and water invasion (S_{org} = 6%).

The using of fluid contact pore volume equations and combining them with the radius of contacts equations has produced the HCV versus depth volume curve (figures C-19 & C-20) for Egyptian reservoir. This has been checked against the same values obtained from logs to get an accurate value for the m ratio (m= 2.589906).

Assuming the production rate for future operations will be 200 STB/D for oil, 2 MMSCFD for Gas, and 600 STB/D for water, the pressure performance for future intervals decreases gradually with time and the predicted values show a good match with those obtained from IMBAL software (figure C-21) for Egyptian field. The first check on water influx (figure C-22) illustrates the similarity between $\mathbf{W_e}$ from MBE and $\mathbf{W_e}$ from the aquifer model. A small difference between two water influx curves and that of IMBAL Software has appeared. The second check on the produced GOR (figure C-23) has also showed a good match between the two curves. As stated above the difference between these curves and that of IMBAL software is due to IMBAL tank assumption and average reservoir gas saturation used, not free gas in un-invaded zone and also. However, the obtained percentage error is less than 5 % not 10 % and it decreases in future intervals to less than 5 % as shown in figure C-24.

CONCLUSIONS

Based on the results and their analysis, the following conclusions are extracted:

(a) An integrated analysis and future prediction for combination drive reservoirs can be done although this requires long equations and a large number of trial and error.

(b) A practical integrated model for analysis and future prediction of combination drive reservoir performance showed a good match with the field cases.

(c) The HCV versus depth curve obtained from the geologists was constructed and a check on the m-ratio can be done.

(d) Future prediction performance is very sensitive to PVT, viscosity and relative permeability correlations.

(e) The integrated model program succeeded in predicting the future performance of the Egyptian field with acceptable matching.

(f) Hydrocarbon recovery from combination drive reservoirs can be increased by gas or water injection as is apparent throughout the results for the Egyptian field.

NOMENCLATURES

A = Area of the reservoir, acres

C_f = Compressibility of the aquifer formation, psi^{-1}

C_w = Compressibility of the water, psi^{-1}

f = Encroachment angle, degree

f_d = Fraction of displacing fluid (Gas or Water) in the flowing stream in the reservoir, fraction

$G_{i(ext)}$ = Cumulative gas injected in excess of that produced from the beginning of pressure maintenance operations to end of the period, Mcf at STD conditions.

G_{pc} = Cumulative gas production for the gas cap, scf

h = Thickness of reservoir, ft

k = permeability of the aquifer, md

k_{rg} = Relative permeability of the reservoir rock to gas, dimensionless

K_{ro} = Relative permeability of the reservoir rock to oil, dimensionless

K_{rw} = Relative permeability of the reservoir rock to water, dimensionless

M = Ratio of initial gas-cap-gas reservoir volumeto initial reservoir oil volume,bbl/bbl

n = Euler constant, dimensionless

N_{tw} is the cumulative volume of oil trapped in the water- invaded zone, STB

N_{tg} is the cumulative volume of oil trapped in the gas-invaded zone, STB

OGIP or G = original free gas-in-place in standard conditions, SCF

OOIP or N = original oil-in-place at surface conditions, STB

PVBOTTOM = pore volume from the bottom to the top of the reservoir, res bbl

PVBWOC =pore volume from bottom water-oil contact to top of reservoir,resbbl

PV_{GOC} = pore volume from gas-oil contact to top of reservoir, res bbl

PV_{OGOC} = pore volume from original gas-oil contact to top of reservoir, res bbl

PV_{OWOC} = pore volume from original water-oil contact to top of reservoir, res bbl

PV_{WOC} = pore volume from water-oil contact to top of reservoir, res bbl

Q_{tD} = dimensionless flow rate

r_a = radius to perimeter of aquifer, ft

r_D = dimensionless radius, ra/re

r_e = radius to perimeter of reservoir, ft

R_{gc} = Current gas/oil contact radius

R_{gi} = Initial gas/oil contact

R_o = Original oil reservoir radius, ft

R_{oc} = Current oil/water contact radius

R_s = Gas solubility, scf/STB

R_{si} = Initial gas solubility, scf/STB

S_{org} = Residual oil saturation in the gas-invaded zone, fraction

S_{orw} = Trapped oil saturation in the water-invaded zone, fraction

S_{wi} = initial or connate water saturation (Swc), fraction

$S_{g\omega}$ = Free gas saturation in un-invaded zone, fraction

t = Time, days

t_D = dimensionless time

W_e = Cumulative water influx, bbl

$W_{i(ext)}$ = Cumulative water injected in excess of that produced from the beginning of pressure maintenance operation to end of the period, bbl

βg = Gas formation volume factor, bbl/scf

B_{gc} = Gas- cap formation volume factor, bbl/SCF

β_{gi} = Initial gas formation volume factor, bbl/scf

β_o = Oil formation volume factor, bbl/STB

β_{oi} = Initial oil formation volume factor, bbl/STB

Δp = Change in reservoir pressure = pi − p, psi

μ_g = Viscosity of reservoir gas, cp

μ_o = Viscosity of reservoir oil, cp

φ = Average porosity of the oil and gas zones, fraction

Ψ = shape factor, dimensionless

Subscripts

ω = Denotes un-invaded oil zone

j, k, n, i = value at a point in time

j-1, k-1, n-1 = value at a previous point in time

d = displacing fluid (water or gas)

REFERENCES

Carter, R. D., & Tracy, G. W. (1960). *An improved method for calculations water influx*, In AIME (Trans.).

Cole, F. (1969). *Reservoir engineering manual*. Houston: Gulf Publishing Company.

Craft, B. C., & Hawkins, M. (1991). *Applied Petroleum Reservoir Engineering* (2nd ed., Revised by Terry, R. E.). Englewood Cliffs, NJ Prentice Hall.

Dardaganian, S. G. (1957). *The displacement of gas by oil in the presence of connate water.* M.S. Thesis, Texas A&M University.

Delauretis, E. F., Yarranton, H. W., & Baker, R. O. (2008, March). Application of material balance and volumetrics to determine reservoir fluid saturations and fluid contact levels. Jour. Pet. Tec., PETSOC-08-03-39-P, *47*(3).

Exxon. (1978). *Reservoir Engineering Manual* (Chapter 6). Production Research Company, Houston, Texas.

Fetkovich, M. J. (1971, July). A simplified approach to water influx calculations-finite aquifer systems. *JPT,* 814-828.

Fetkovich, M. J., Fetkovich, E. J., & Fetkovich, M. D. (1994, September 25-28). Useful concepts for decline curve forecasting, reserve estimation, and analysis (paper SPE 28628 presented at the 1994 Annual Technical Conference and Exhibition). *New Orleans*.

Fetkovich, M. J., Fetkovich, E. J., & Fetkovich, M. D. (1994, September 25-28). *Useful concepts for decline curve forecasting, reserve estimation, and analysis* (paper SPE

28628 presented at the 1994 Annual Technical Conference and Exhibition), New Orleans.

Havlena, D., & Odeh, A. S. (1963, August). The material balance as an equation of a straight line. *JPT, 896-900*.

Havlena, D., & Odeh, A. S. (1964, July). The material balance as an equation of a straight line. Part II-Field Cases. *JPT*, 815-822.

Hurst, W. (1943). *Water influx into a reservoir and its application to the equation of volumetric balance* (Vol. 151, pp. 57), In AIME (Trans.).

Kirby, J. E. Jr., Stamm, H. E., & Schnitz, L. B. (1956). *Calculation of the depletion history and future performance of a gas-cap-drive reservoir*, In AIME (Trans.). SPE-671-G.

Klins, M. A., Bouchard, A. J., & Cable, C. L. (1988, February). A polynomial approach to the van everdingen-hurst dimensionless variables for water encorachment. *SPERE*, 320-26.

Naar, J., & Henderson, J. H. (1961). *An imbibition model - its application to flow behavior and the prediction of oil recovery*. SPEJ, 61.

Saad T, Saleh. (1990). *An improved model for the development and analysis of partial-water drive oil reservoirs* (Paper NO. CIM/SPE, pp.90-38). University Of Alska, Falrbanks.

Schilthuis, R. (1936). *Active oil and reservoir energy* (pp.37, 118), In AIME (Trans.).

Smith, C. R., Tracy, G. W., & Farrar, R. L. (1992). Applied reservoir engineering, *2*.

Tarek, A. (2006). *Reservoir engineering handbook* (3rd ed.).

Tracy, G. (1955). Simplified form of the MBE (Vol. 204, pp. 243-246), In AIME (Trans.).

Van Everdingen, A., & Hurst, W. (1949). The application of the Laplace transformation to flow problems in reservoirs, In AIME (Trans.). *186*, 305.

Welge, H. L. (1952). Simplified method for calculating oil recoveries by gas or water drive. In AIME (Trans.). *195*, 91.

Wooddy, L. D Jr., & Moscrip, R III. (1956). Performance calculations for combination drive reservoirs, In AIME (Trans.). *207*, 128.

APPENDIX (A) MODEL PROCEDURES

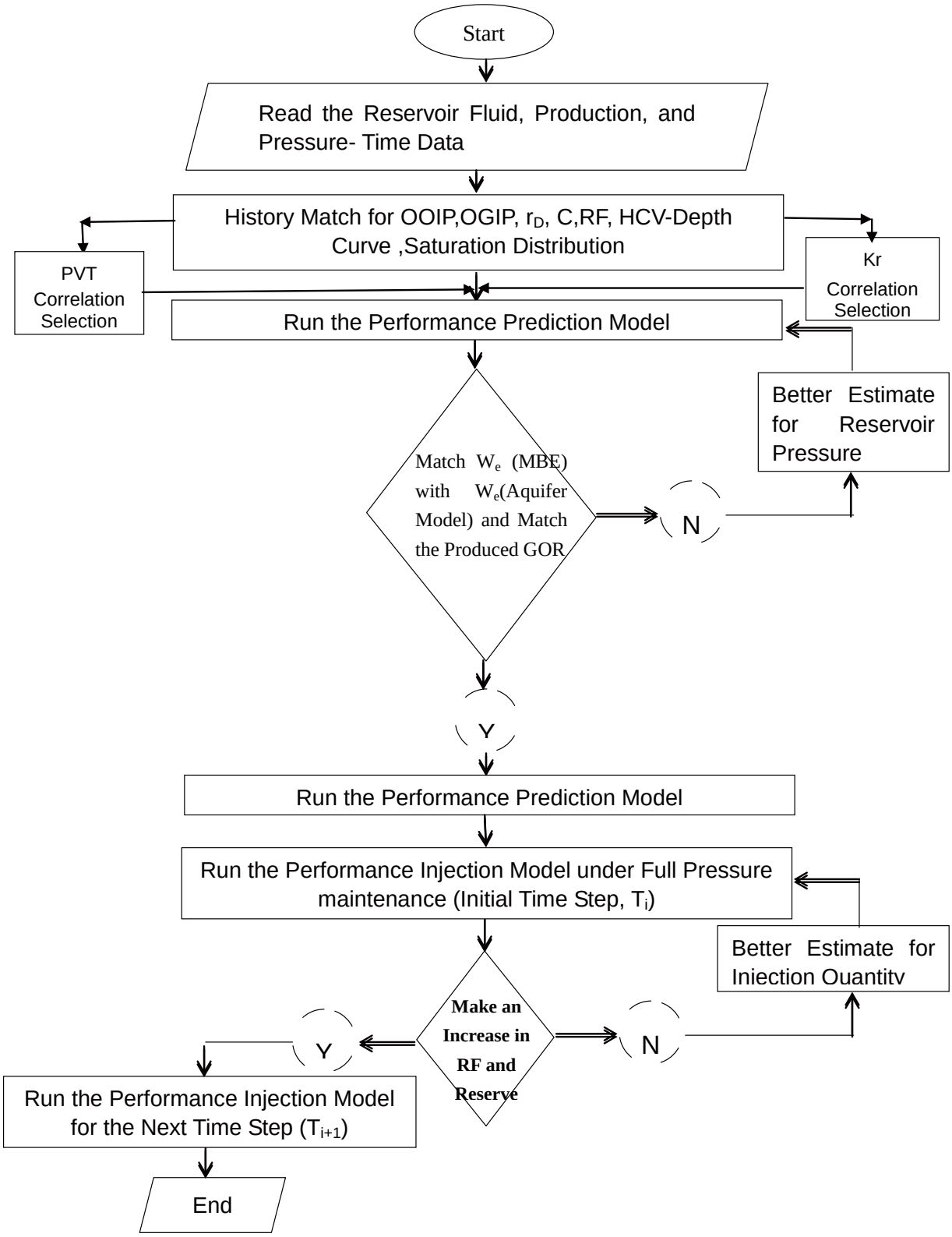

Figure A-1
Flow Diagram for General Integrated Model Procedures

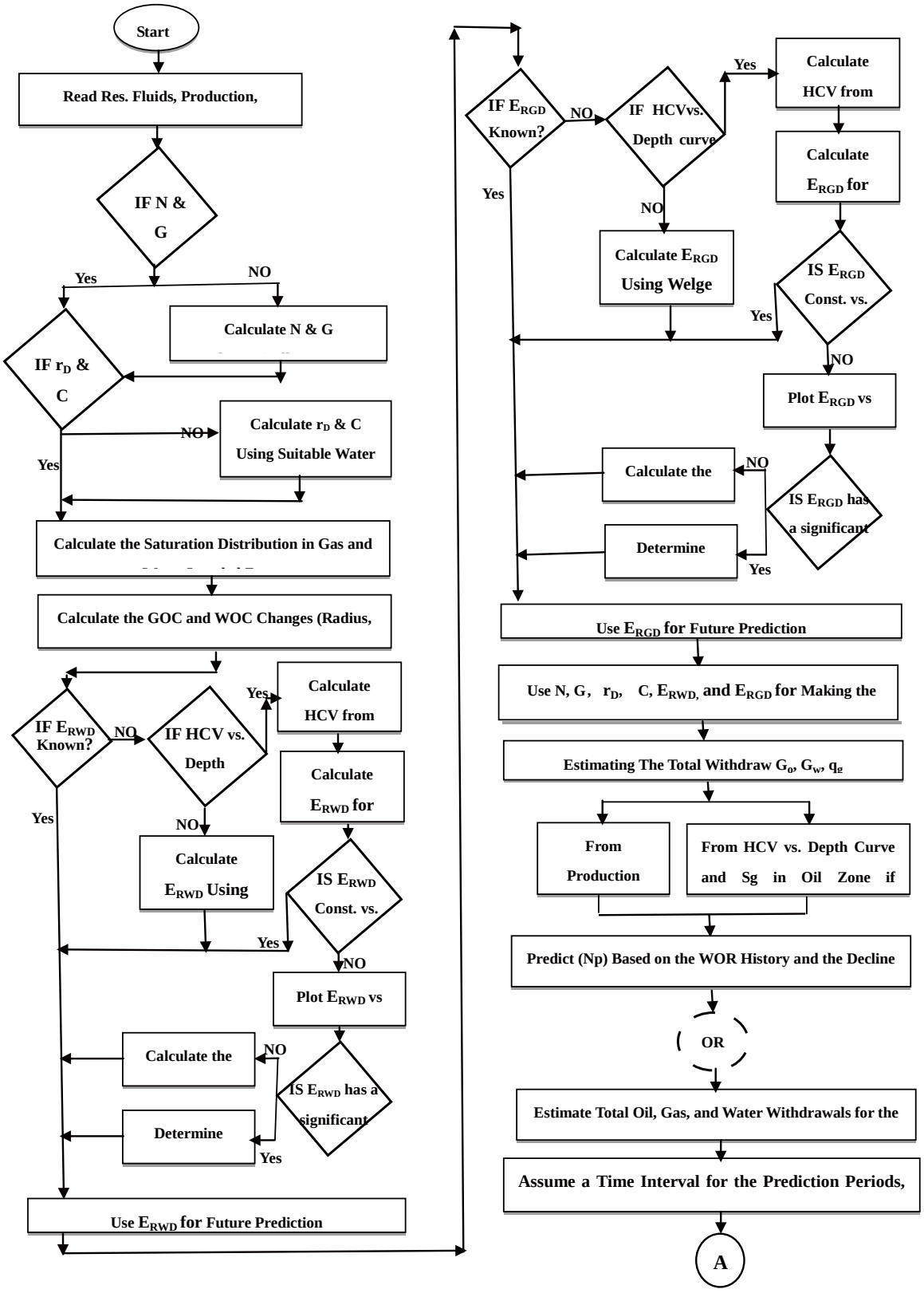

Figure A-2
Flow Diagram for History Match and Future Performance Predicting of Combination Drive Reservoirs

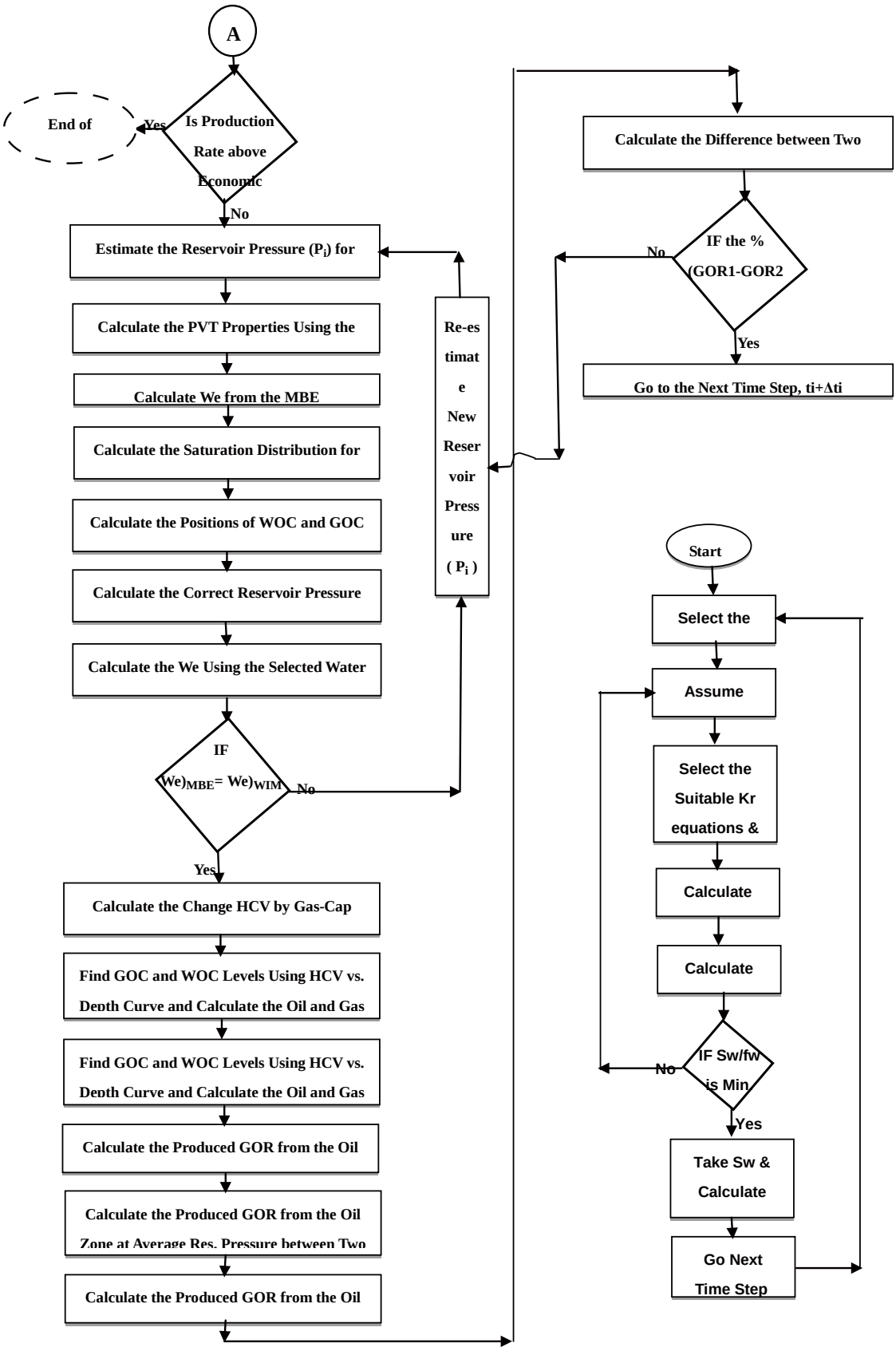

Figure A-3
Flow Diagram for Welge Method in Case of Water Displacement

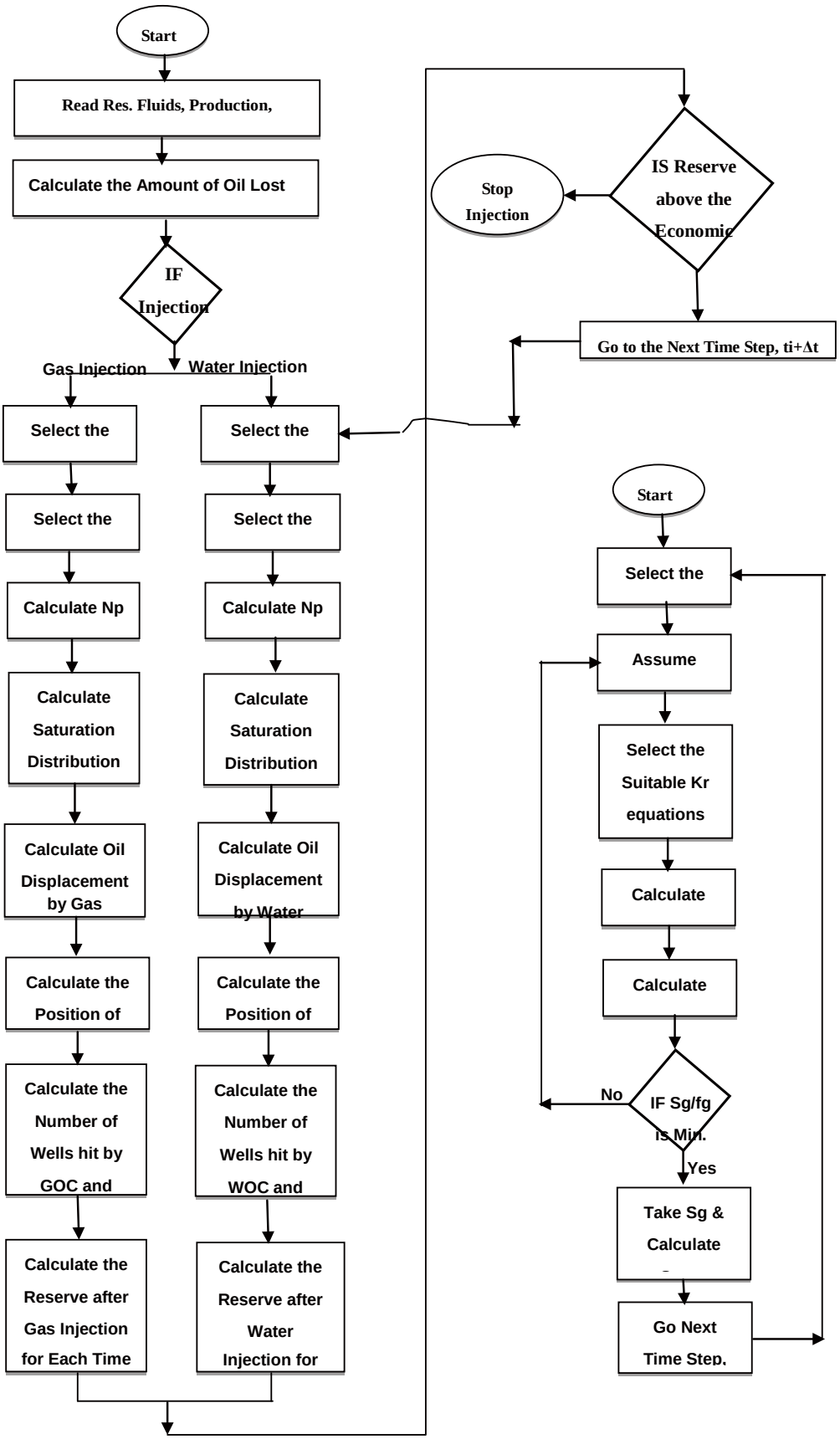

Figure A-4
Flow Diagram for Predicting the Performance of Combination Drive Reservoir during Water and Gas Injection

APPENDIX (B) CASES FIELD DATA

Table B-1
Pressure Production History for Case (1)

Time (days)	Reservoir Pressure @ Datum, Psia	Cumulative Production		
		Oil,MMSTB	Gas,MMMSCF	Water(MMbbl)
0	2400	0	0	0
182.5	2380	2.1	2.11	0
365	2320	9.7	9.6	0
547.5	2260	19	18.62	0
730	2180	30	30.55	0
912.5	2100	42	47.12	0

Table B-2
Reservoir Rock and Fluid Data for Case (1)

Oil zone		Gas Cap zone		Aquifer	
Voi, MM bbl	725	**Vgi, MM bbl**	219.27	r_D,	10
N, MMSTB	438.86	**G , MMSCF**	191.17	**kw, md**	155
Swi, % PV	20	**Kg, md**	155	**φ,%**	20
γ_o	0.63	γ_g	0.13	C_{f+w} , Psi^{-1}	6x10^{-6}
α_d, degrees	6	α_d, degrees	6	μ_w, cp	0.37
R_{WOC}, ft	10700	R_{GOC}, ft	4950	γ_w	1.13
h_o, ft	100	h_g, ft	100		

Table B-3
Pressure Production History for the Egyptian Field Case (3)

t(days)	p(psi)	Np(MMSTB)	Gp(OIL Zone)	Gp(Gas-Cap)	Gp(BSCF)	Wp(MMSTB)
0	2919	0	0	0	0	0
182.5	2902	0.107956	0.101838	0	0.101838	0.002893
365	2870	0.28372	0.3764284	0	0.3764284	0.013937
547.5	2838	0.599151	0.749953693	0	0.749953693	0.029867
730	2806	0.863278	1.04998925	0	1.04998925	0.049301
912.5	2774	1.090988	1.342504304	0	1.342504304	0.074478
1095	2742	1.263502	1.605693588	0	1.605693588	0.106082
1277.5	2711	1.417812	2.023867746	0	2.023867746	0.14898361
1460	2679	1.540153	2.315363686	0	2.315363686	0.23125779
1642.5	2647	1.630655	2.803896276	0	2.803896276	0.30684446
1825	2615	1.702742	3.657525508	0	3.657525508	0.42164046

Table B-4
Reservoir Rock and Fluid Data for the Egyptian Field Case (3)

Oil zone		Gas Cap zone		Aquifer	
Voi, MM bbl	10.8384	**Vgi, MM bbl**	28.07044	r_D,	---
N, MMSTB	-	**G , MMSCF**	-	**kw, md**	4902
Swi, % PV	23	**Kg, md**	4902	**φ,%**	23
γ_o	0.7995	γ_g	0.712	C_{f+w} , Psi^{-1}	6x10^{-6}
α_d, degrees	6	α_d, degrees	6	μ_w, cp	0.4
A_{WOC}, ft^2	2840022.08	A_{GOC}, ft^2	4839073.79	γ_w	1.0545
h, ft	22				

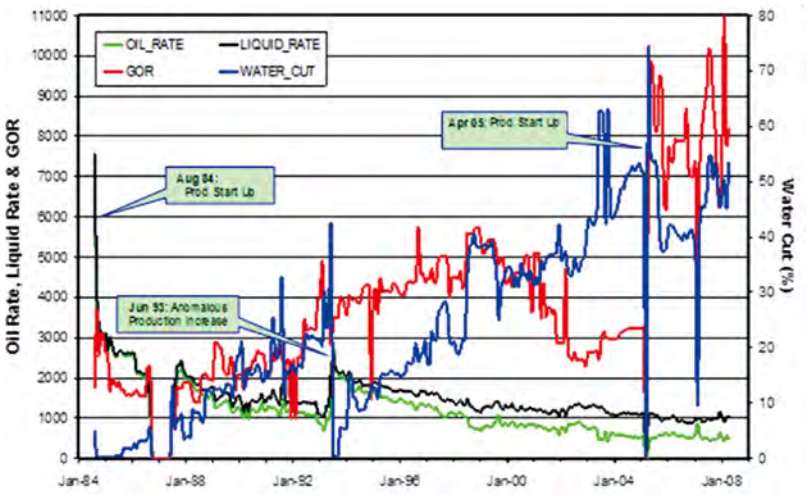

Figure B-1
The Production History of the Egyptian Combination Drive Field- Case (2)

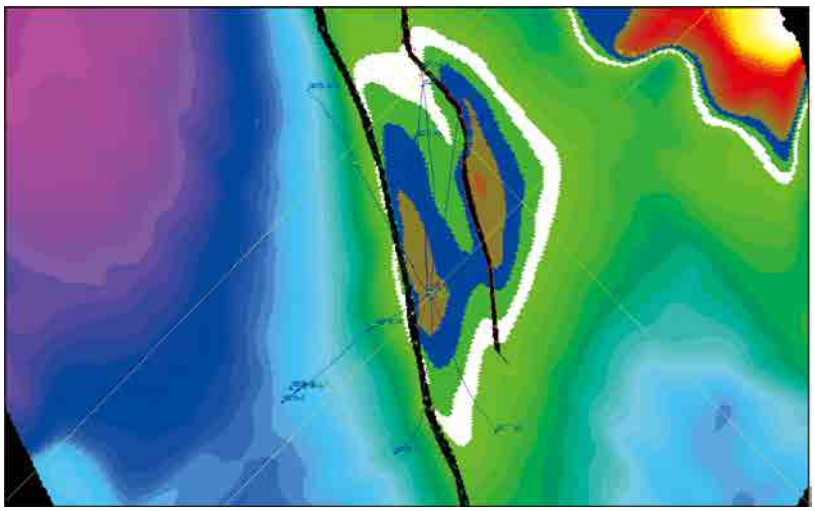

Figure B-2
Depth Map of the Egyptian Combination Drive Oil Field –Case (2)

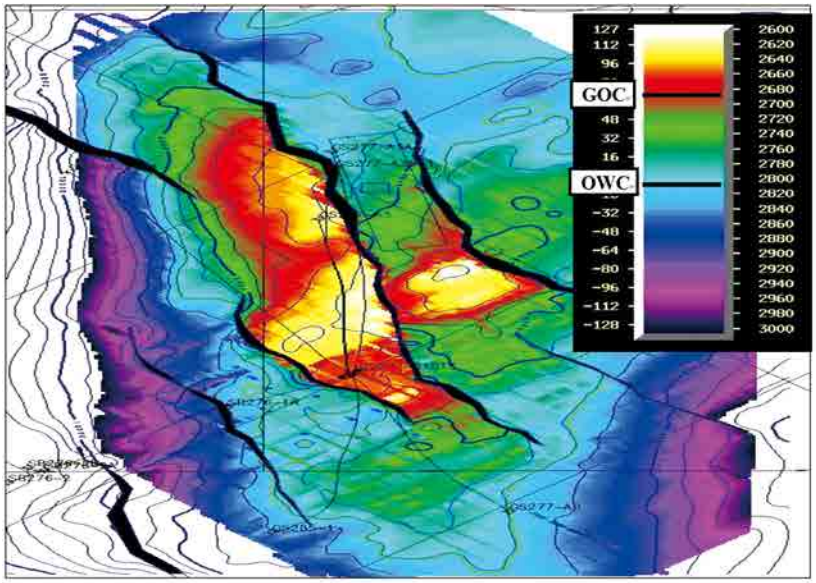

Figure B-3
Depth Structure Map of the Egyptian Combination Drive Oil Field –Case (2)

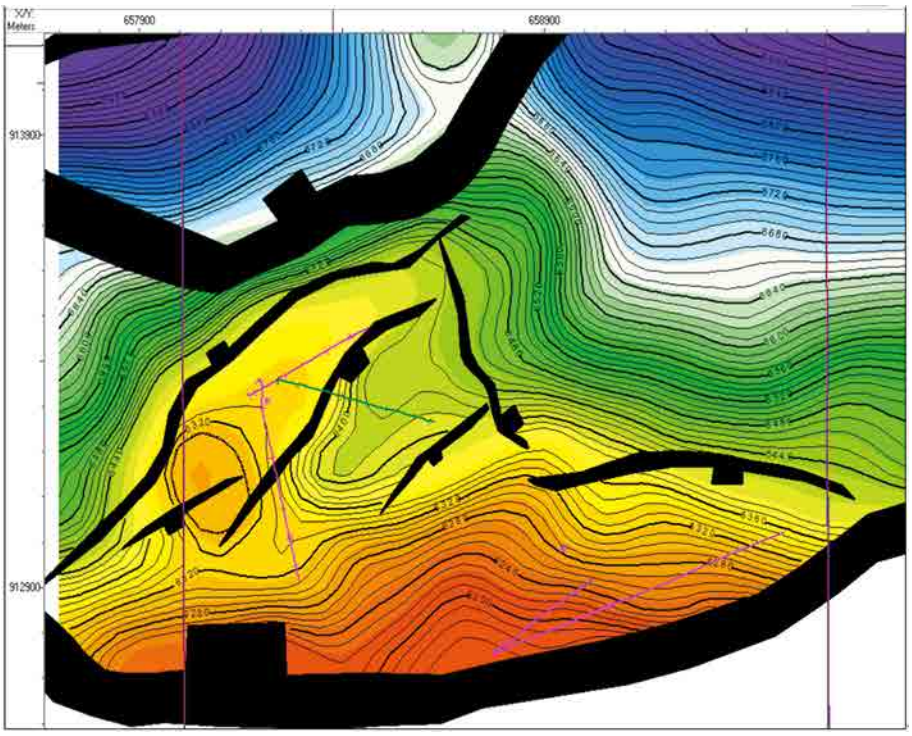

Figure B-4
Structure Depth Contour Map for the Egyptian Oil Field- Case (3)

APPENDIX (C) MODEL RESULTS

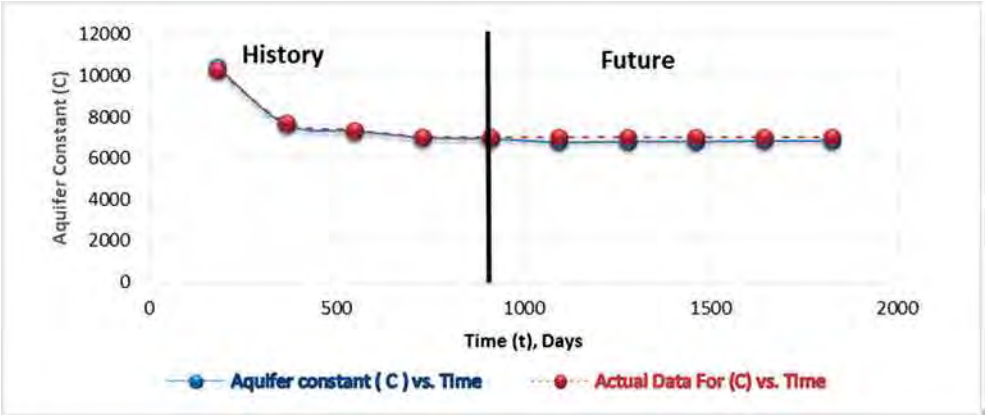

Figure C-1
Aquifer Constant (C) versus Time Case (1).

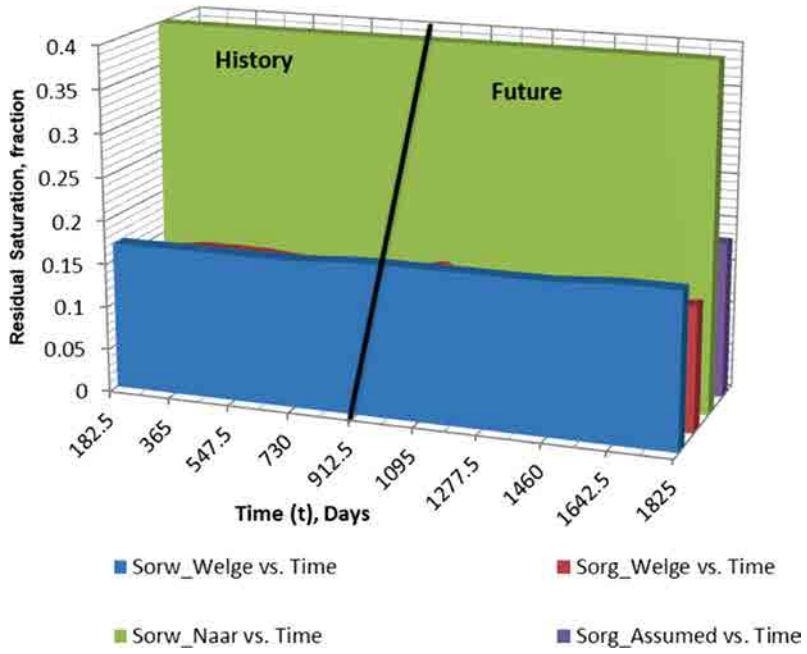

Figure C-2
Residual Saturations in Invaded Zones versus Time Case (1).

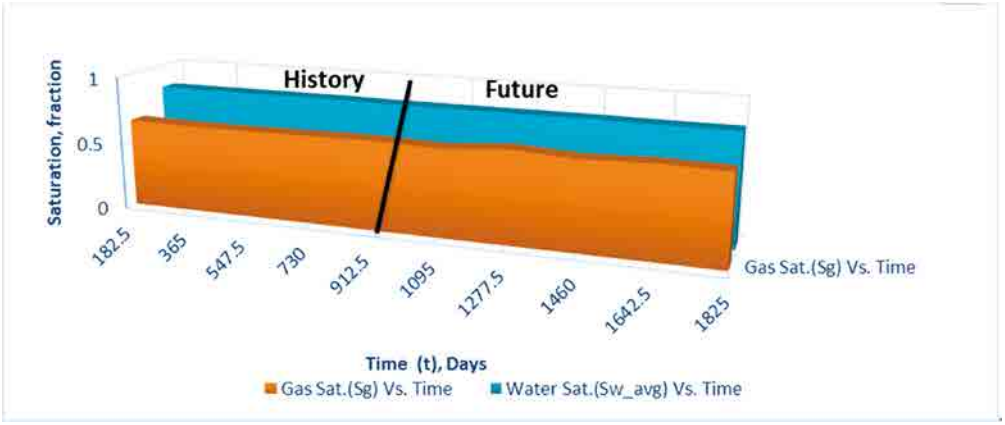

Figure C-3
Average Gas Saturation (S_{gavg}) in Gas Invaded Zone and Average Water Saturation (S_{wavg}) in Water Invaded Zone versus Time Case (1).

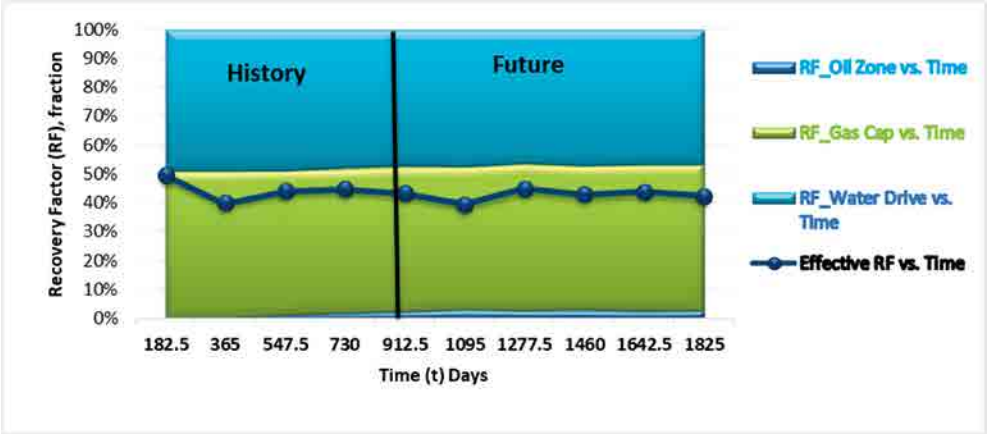

Figure C-4
Recovery Factor versus Time Case (1).

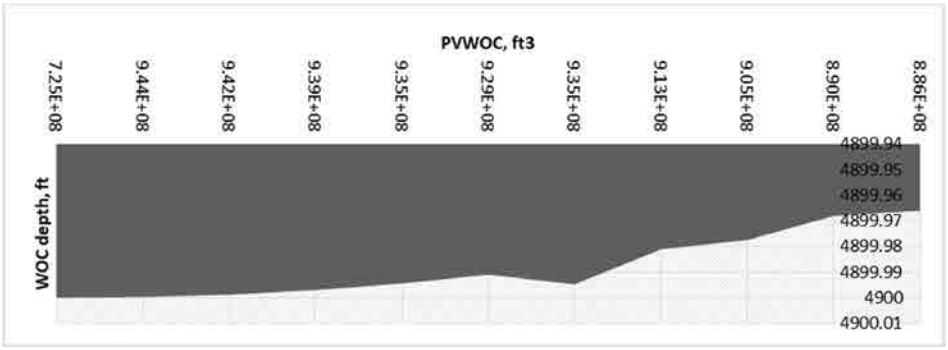

Figure C-5
Water Oil Contact (WOC) Depth versus Pore Volume Above Water Oil Contact (PVWOC) Case (1).

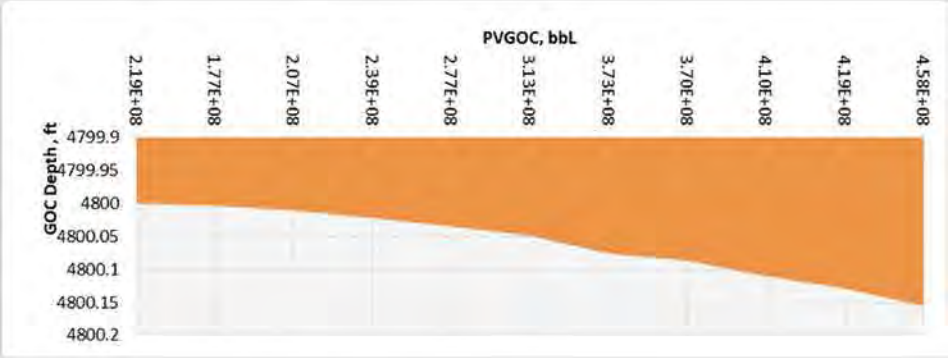

Figure C-6
Gas Oil Contact (GOC) Depth versus Pore Volume Above Gas Oil Contact (PV_{GOC}) Case (1).

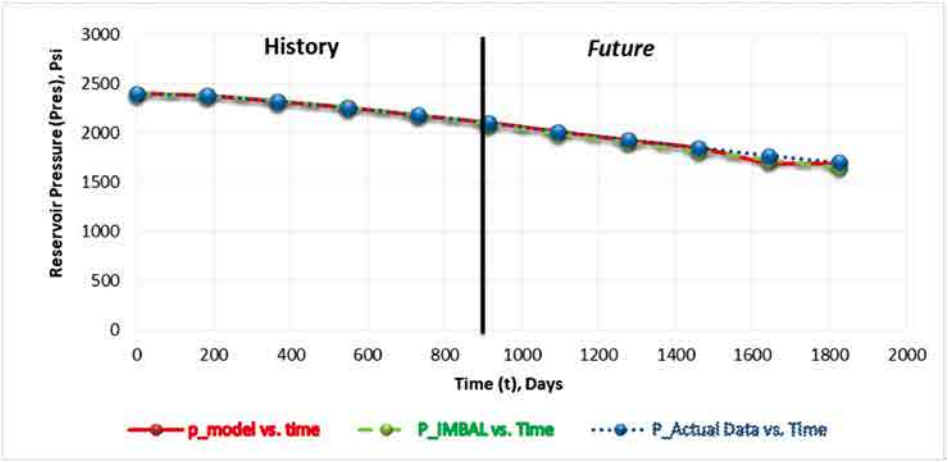

Figure C-7
Reservoir Pressure versus Time Case (1).

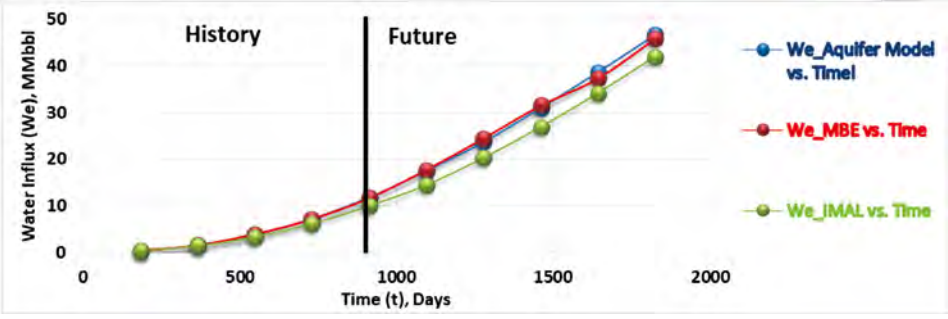

Figure C-8
Water Influx versus Time Case (1).

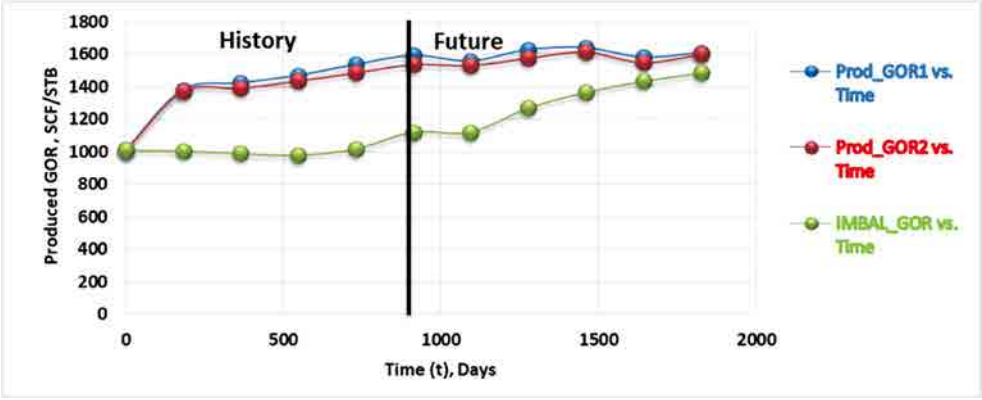

Figure C-9
The Produced GOR versus Time Case (1).

Figure C-10
The Error Percentage of GOR versus Time Case (1).

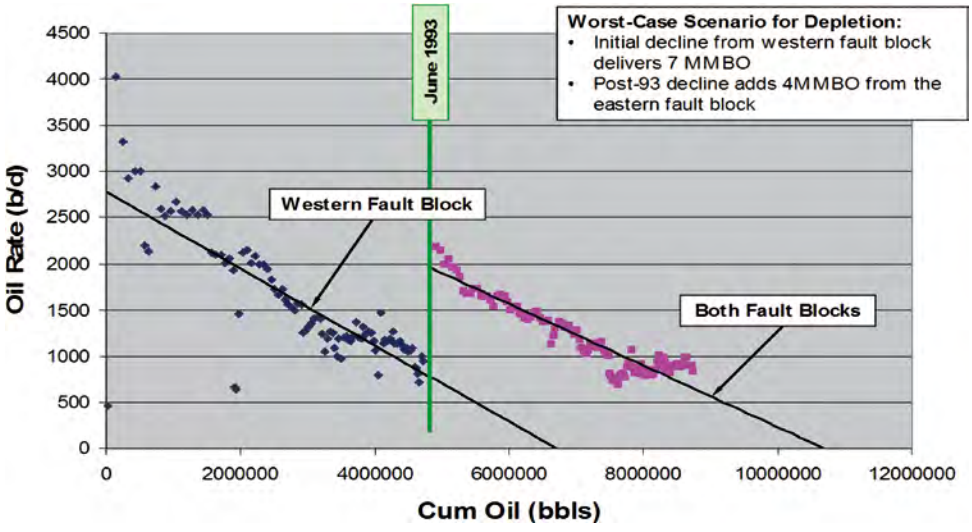

Figure C-11
The Oil Rate versus Cumulative Oil for the Egyptian Combination Drive Oil Field – Case (2)

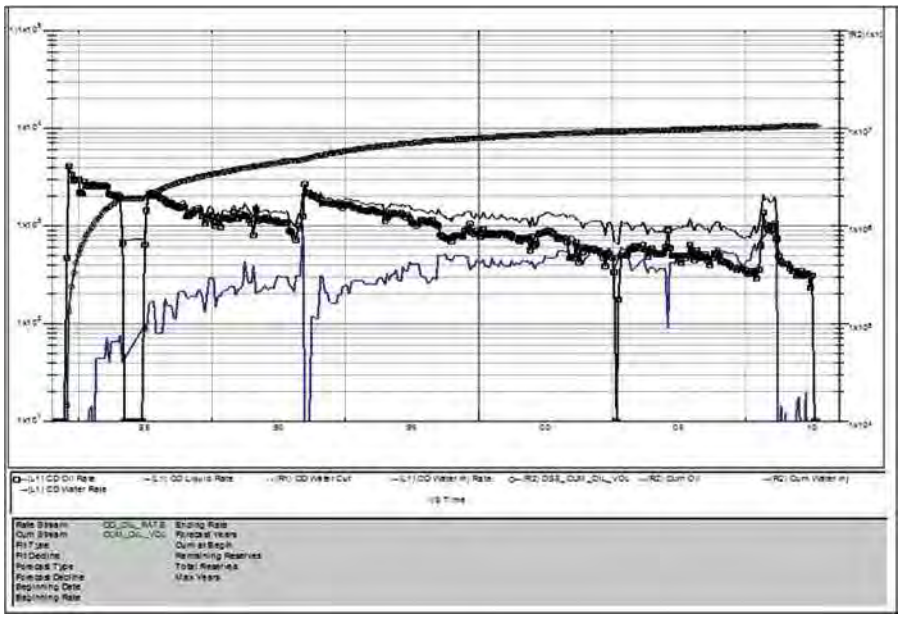

Figure C-12 (A)
The Decline Forecast-rate Time of the Egyptian Combination Drive Oil Field – Case (2)

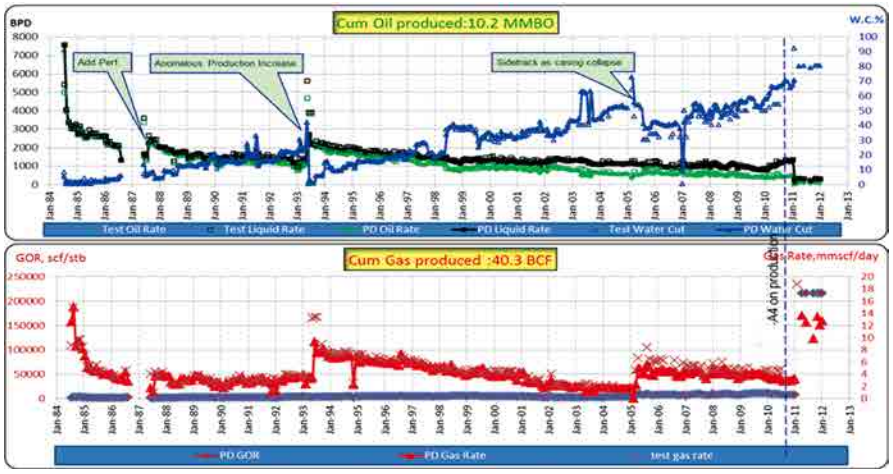

Figure C-12 (B)
The Decline Forecast-Rate Time of the Egyptian Combination Drive Oil Field – Case (2)

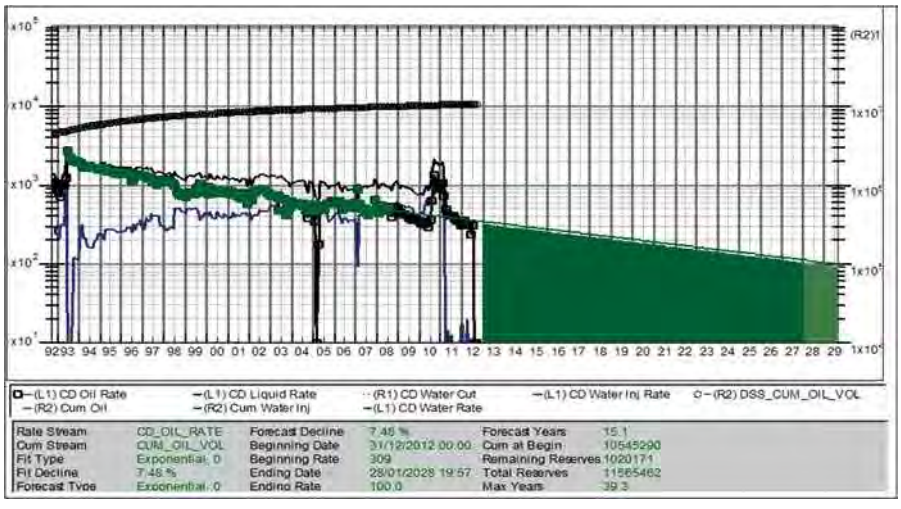

Rate Stream	CD_OIL_RATE	Forecast Decline	7.48 %	Forecast Years	15.1
Cum Stream	CUM_OIL_VOL	Beginning Date	31/12/2012 00:00	Cum at Begin	10545290
Fit Type	Exponential, 0	Beginning Rate	309	Remaining Reserves	1020171
Fit Decline	7.48 %	Ending Date	28/01/2028 19:57	Total Reserves	11565462
Forecast Type	Exponential, 0	Ending Rate	100.0	Max Years	39.3

Figure C-13
The Decline Forecast-Rate Time of the Egyptian Combination Drive Oil Field – Case (2)

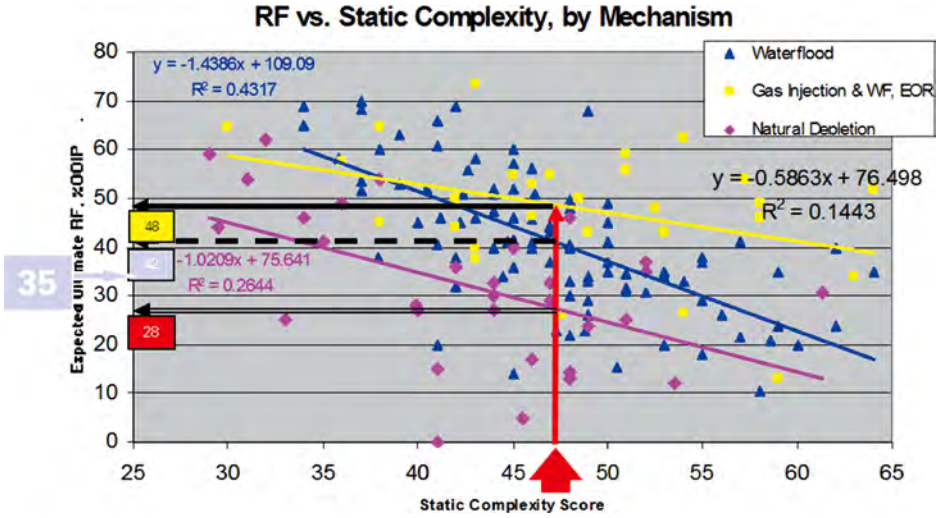

Figure C-14
The Expected Ultimate RF During Injection of the Egyptian Combination Drive Oil Field – Case (2)

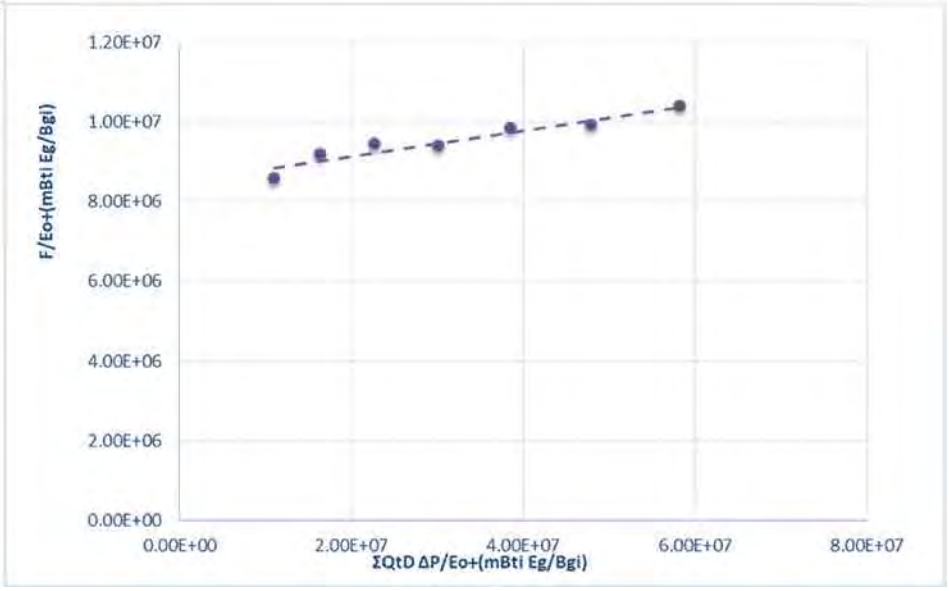

Figure C-15
Havlena and Odeh Approach for the Egyptian Oil Field for Determining the OOIP and Aquifer Constant – Case (3)

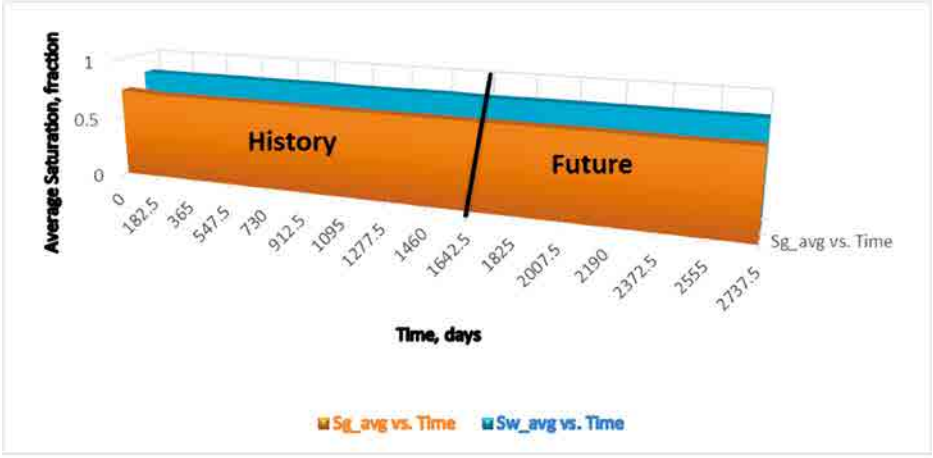

Figure C-16
Average Gas Saturation (S_{gavg}) in Gas Invaded Zone and Average Water Saturation (S_{wavg}) in Water Invaded Zone versus Time for the Egyptian Oil Field –Case (3)

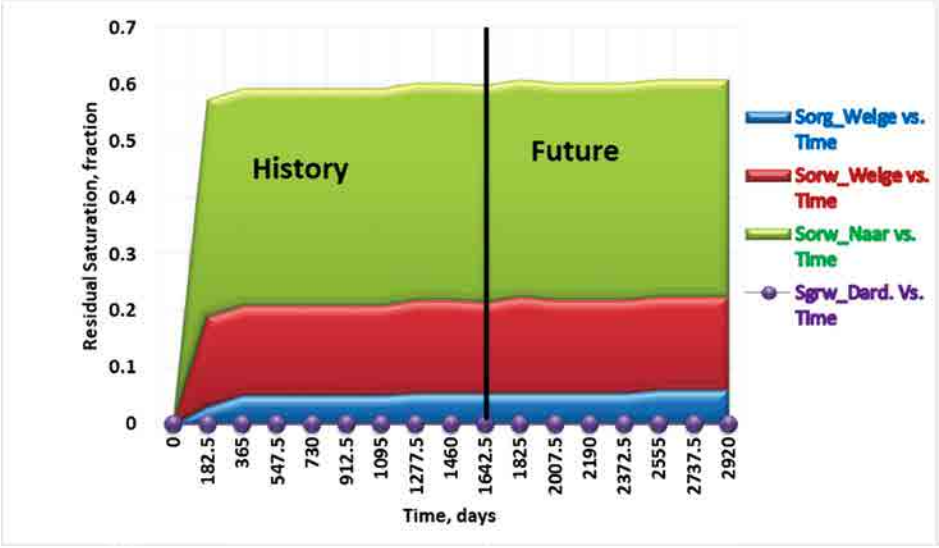

Figure C-17
Residual Saturations versus Time for the Egyptian Oil Field–Case (3)

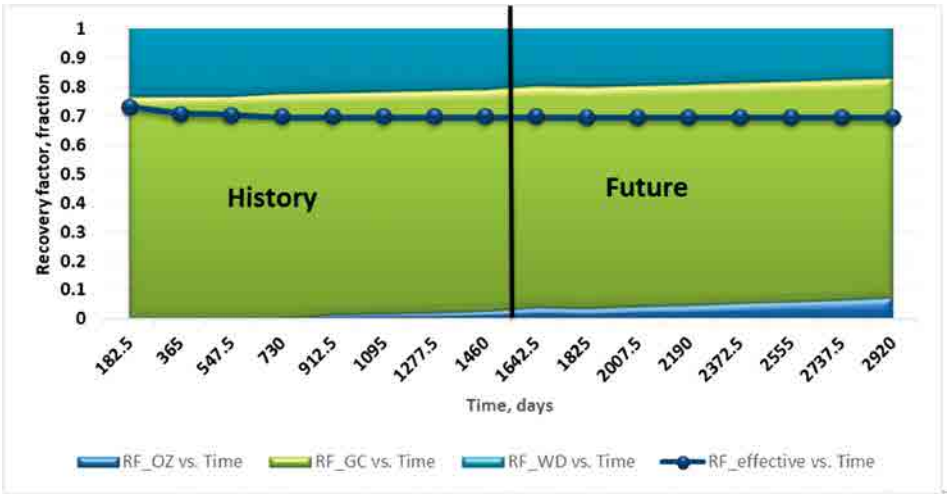

Figure C-18
Recovery Factor versus Time for the Egyptian Oil Field–Case (3)

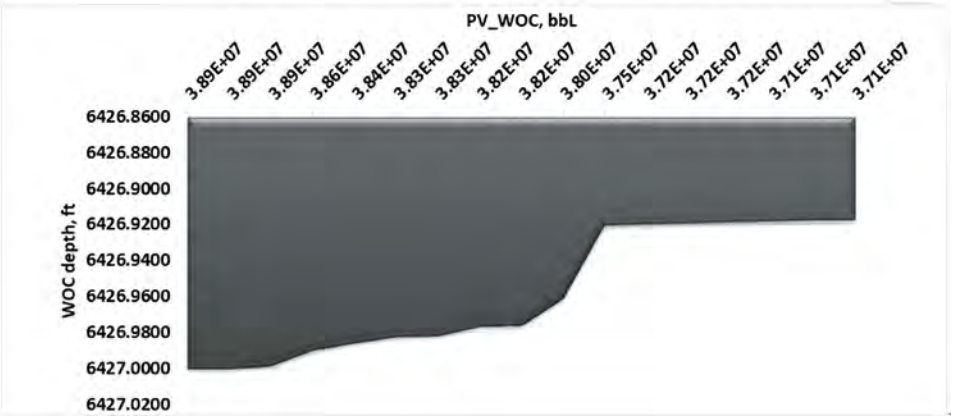

Figure C-19
Water Oil Contact (WOC) Depth versus Pore Volume Above Water Oil Contact (PV_{WOC}) for the Egyptian Oil Field–Case (3)

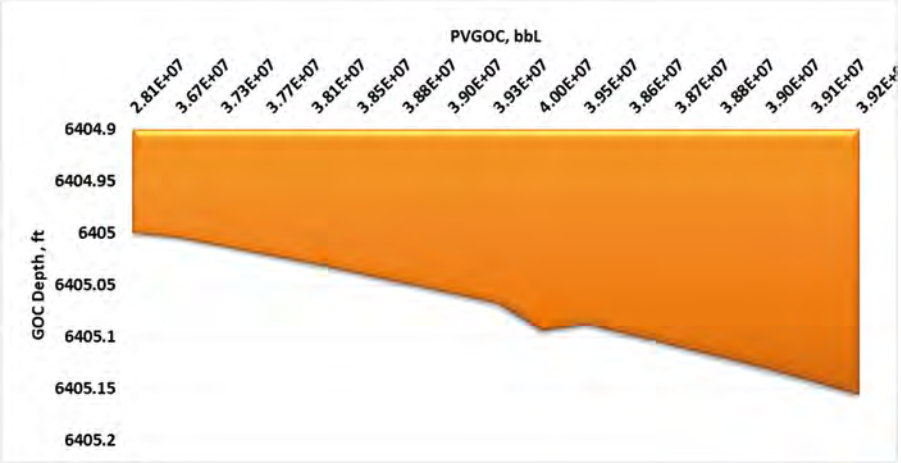

Figure C-20
Gas Oil Contact (GOC) Depth versus Pore Volume Above Gas Oil Contact (PV_{GOC}) for the Egyptian Oil Field–Case (3)

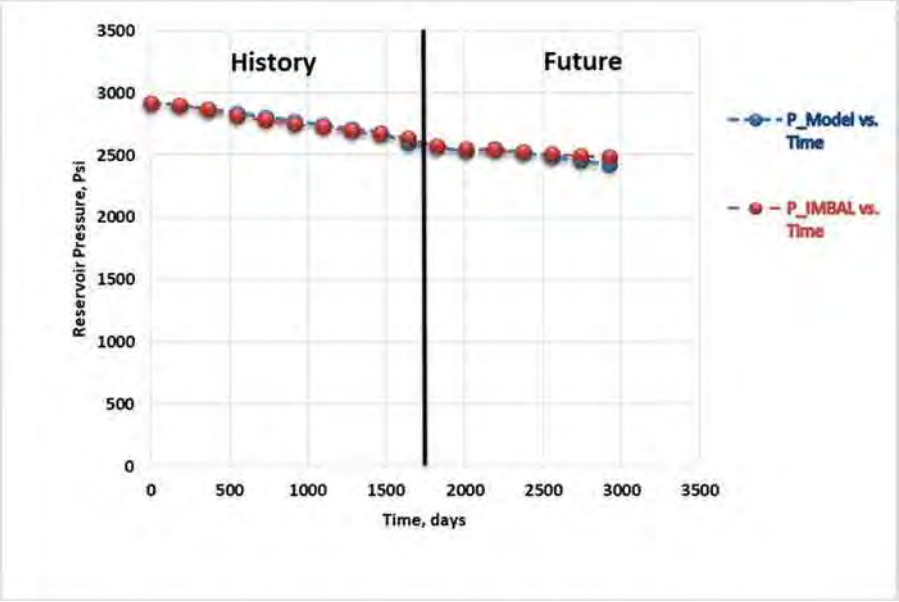

Figure C-21
Reservoir Pressure versus Time for the Egyptian Oil Field–Case (3)

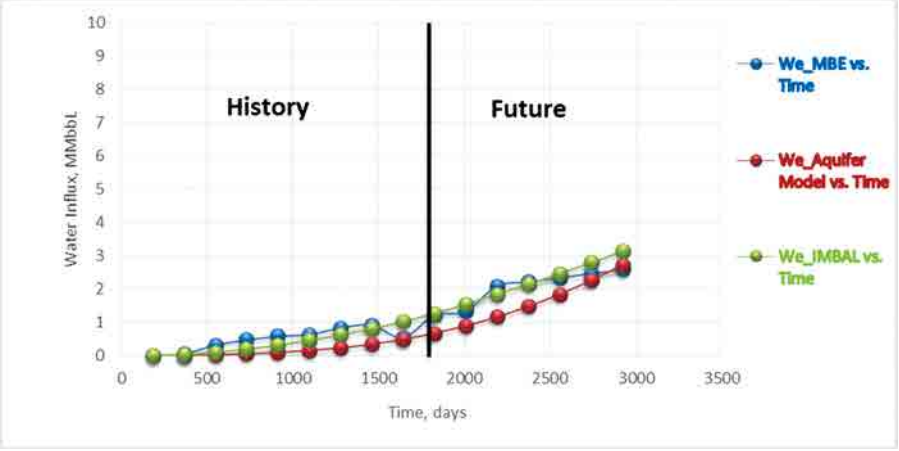

Figure C-22
Water Influx versus Time for the Egyptian Oil Field–Case (3)

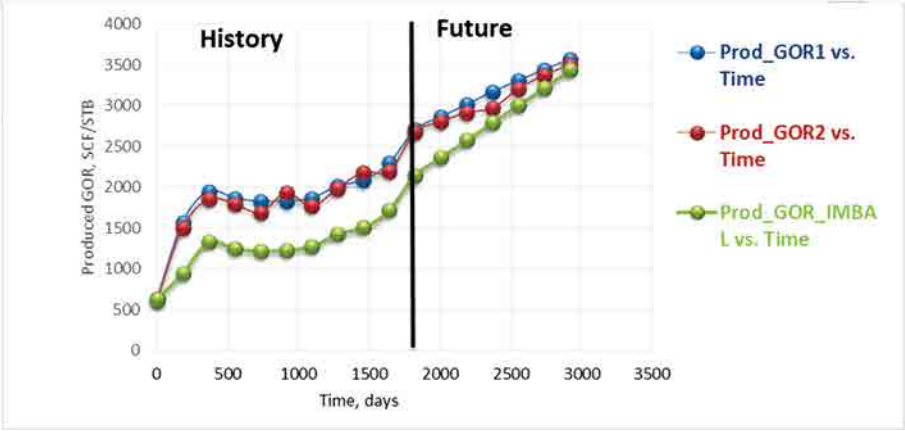

Figure C-23
The Produced GOR versus Time for the Egyptian Oil Field–Case (3)

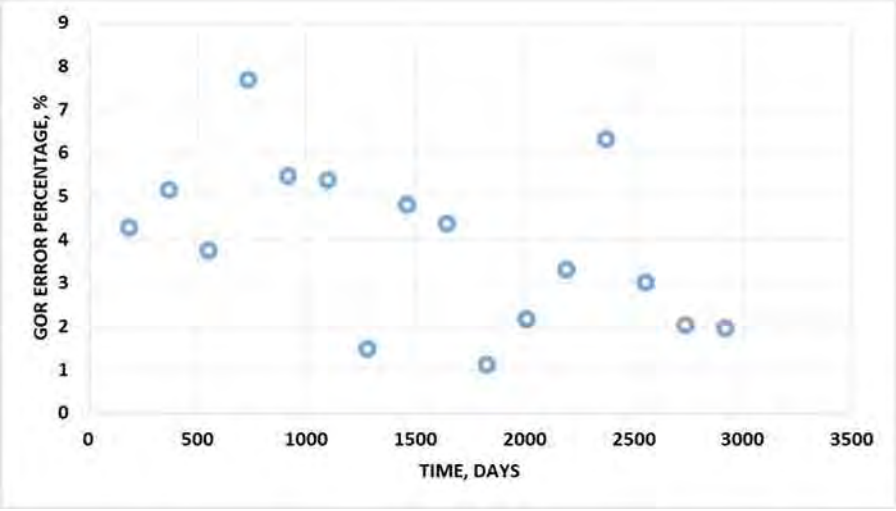

Figure C-24
The Error Percentage of GOR versus Time for the Egyptian Field–Case (3)